Journal of Applied Geophysics 103 (2014) 152–160

Contents lists available at ScienceDirect

Journal of Applied Geophysics

journal homepage: www.elsevier.com/locate/jappgeo

The ratio apparent resistivity definition of rectangular-loop TEM

Zhou NanNan *, Xue GuoQiang

Key Laboratory of Mineral Resources, Institute of Geology and Geophysics, Chinese Academy of Science, Beijing 100029, China

ARTICLE INFO

Article history:
Received 18 March 2013
Accepted 20 January 2014
Available online 5 February 2014

Keywords:
Rectangular loop
Uniform distribution
Ratio response
Translation and scaling
Apparent resistivity
Time domain

ABSTRACT

The conventional method for computing the apparent resistivity of any location within a rectangular loop is to use the associated vertical magnetic field or its time derivative by a well-developed central-loop equation. For central part of the loop, this definition of apparent resistivity is accurate, and the survey configuration is designated as modified central-loop TEM. However, when applied to the non-central part of the rectangular loop that often demonstrates uneven distribution of magnetic field the use of this equation runs the risk of producing computational errors.

Instead of the uneven distribution of vertical magnetic field, ratio response of the orthogonal horizontal field components has a uniform field distribution. Furthermore, the decay curves of ratio response reveal the properties of translation and scaling. By examining the decay curves for different resistivity, a new definition of ratio apparent resistivity is proposed, which is applicable for any point in a loop with the uniform distribution of ratio response. With the proposed explicit function between ratio response and apparent resistivity, our new algorithm avoids the time-consuming iteration by solving a non-linear equation. Both theoretical modeling and real data example indicate the added value of our method on computational efficiency and accuracy.

1. Introduction

Apparent resistivity can be computed by comparing the real field to the homogeneous half-space model. However, transient electromagnetic field of rectangular loop is complicated and often affected by geo-electric parameter, observation time and device. Therefore, there is no explicit function between transient response and apparent resistivity (Li et al., 2007; Qi et al., 2011; Shi et al., 2009; Ward and Hohmann, 1991; Xue et al., 2012; Zhou et al., 2011).

Central-loop and coincident-loop configurations are the most popular systems of TEM and the apparent resistivity for these configurations has been researched widely. Lee and Lewis (1974) presented the asymptotic formula of apparent resistivity; Spies and Raiche (1980) defined the apparent resistivity in the form of approximate finite series, and then developed an iteration algorithm of the late-time apparent resistivity for coincident loop (Raiche and Spies, 1981); Christensen (1995) further improved this algorithm and proposed a fitting method for computing the all-time apparent resistivity.

Based on the developed research on apparent resistivity of central-loop and coincident-loop TEM, most previous papers have used a circular loop to simulate the response and calculate the apparent resistivity of rectangular loop (Lee and Lewis, 1974; Spies and Raiche, 1980). For the central points of rectangular loop, the difference between circular loop and rectangular loop with equal magnetic moment is very subtle (Ward and Hohmann, 1991). However, for the non-central points, using circular loop to simulate rectangular loop will cause some computational error, especially at the early stage (Xue et al., 2012).

In order to resolve this major limitation, other components of electromagnetic field for rectangular loop are required to be studied. The field equations of rectangular loop are derived as the integral of the corresponding component of electric dipole. The response of electric dipole can be separated into current-source term and charge-source term (grounded term). For the rectangular loop, the charge-source term can be ignored and the response can be integrated by current-source term of electric dipole. In contrast to the uneven distribution of vertical magnetic field, the ratio response distribution of orthogonal field of horizontal component of both electric field and magnetic field is uniform. This paper first presents a new definition of apparent resistivity, which is based on the observed uniform distribution of ratio response of orthogonal horizontal electric field and the perpendicular horizontal magnetic field. According to the uniform characteristic of ratio response, the apparent resistivity definition of any point in loop will also be valid for other points in loop, which could significantly improve the computational efficiency. Next, apparent resistivity expression is developed by the translation and scaling property of the ratio response curves for different resistivity. Finally, the formula is verified through computing apparent resistivity of other points in loop for classic geo-electric model.

* Corresponding author at: Beitucheng Western Road 19th, Chaoyang District, Beijing, China.

http://dx.doi.org/10.1016/j.jappgeo.2014.01.015
0926-9851/

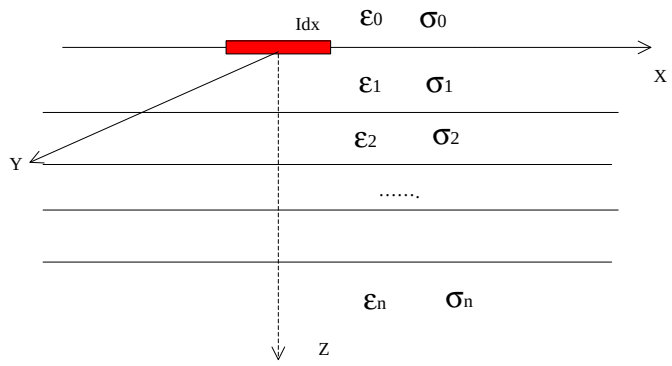

Fig. 1. Sketch map of electric dipole on layered ground.

2. Forward calculation

2.1. Response of horizontal electric dipole

The electric and magnetic fields of rectangular loop can be calculated by integrating the generated field by electric dipole (Fig. 1). The response created by horizontal electric dipole has already been well studied, and this field can be separated into current-source term and grounded term (Kauahikaua, 1978). The grounded term vanishes after integration. Therefore, only the current fields of X-directed electric dipole are needed for field simulation (Ward and Hohmann, 1991):

$$E_x = -\frac{\hat{z}_0 Idl}{4\pi}\int_0^\infty (1+r_{TE})\frac{\lambda}{u_0}J_0(\lambda r)d\lambda \tag{1}$$

$$H_y = -\frac{Idl}{4\pi}\int_0^\infty (1-r_{TE})\lambda J_0(\lambda r)d\lambda \tag{2}$$

$$H_z = \frac{Idl}{4\pi}\frac{y}{r}\int_0^\infty (1+r_{TE})\frac{\lambda^2}{u_0}J_1(\lambda r)d\lambda \tag{3}$$

$$E_y = E_z = H_x = 0 \tag{4}$$

$$r_{TE} = \frac{Y_0-\hat{Y}_1}{Y_0+\hat{Y}_1} \quad r_{TM} = \frac{Z_0-\hat{Z}_1}{Z_0+\hat{Z}_1}$$

where, $Y_0 = \frac{u_0}{\hat{z}_0}$, $Z_0 = \frac{u_0}{\hat{y}_0}$, $\hat{z}_0 = i\omega\mu_0$, $\hat{y}_0 = i\omega\varepsilon_0$.

For the N-layer model (Ward and Hohmann, 1991)

$$\hat{Y}_n = Y_n\frac{\hat{Y}_{n+1}+Y_n\tanh(u_n h_n)}{Y_n+\hat{Y}_{n+1}\tanh(u_n h_n)};\ \hat{Y}_n = Y_n;\ \hat{Z}_n$$
$$= Z_n\frac{\hat{Z}_{n+1}+\hat{Z}_n\tanh(u_n h_n)}{Z_n+\hat{Z}_{n+1}\tanh(u_n h_n)};\ \hat{Z}_n = Z_n$$

where, $Y_n = \frac{u_n}{\hat{z}_n}$, $Z_n = \frac{u_n}{\hat{y}_n}$; $u_n = \left(k_x^2+k_y^2-k_n^2\right)^{1/2}$, $k_n^2 = -\hat{z}_n\hat{y}_n = \omega^2\mu_n\varepsilon_n - i\omega\mu_n\sigma_n$, $k_x^2+k_y^2 = \lambda^2$.

With the assumptions that the earth is homogeneous half space and the frequency is low enough, the expressions could be simplified. Just like the derivation process of time-domain derivative of vertical magnetic field presented in Ward and Hohmann (1991), the time-domain fields of current-source term can be simplified into

$$h_z = \frac{Idsy}{4\pi\rho^3}\left\{\left(1-\frac{3}{2\theta^2\rho^2}\right)erf(\theta\rho)+\frac{3}{\theta\rho}\frac{1}{\sqrt{\pi}}e^{-\theta^2\rho^2}\right\} \tag{5}$$

$$h_y = \frac{Ids}{2\pi\rho^2}I_1\left(\frac{\theta^2\rho^2}{2}\right)e^{-\theta^2\rho^2/2} \tag{6}$$

$$e_x = -\frac{Ids}{2\pi\sigma\rho^3}\left[erf(\theta\rho)-\frac{2}{\sqrt{\pi}}\theta\rho e^{-\theta^2\rho^2}\right] \tag{7}$$

where, $\theta = \left(\frac{\mu\sigma}{4t}\right)$, σ is the conductivity of the earth, and ρ is the distance from the receiver to the source.

2.2. Electric and magnetic fields of rectangular loop

A diagrammatic explanation of calculating the EM response for the rectangular loop is illustrated in Fig. 2. The center of the loop is at (0, 0), and its dimensions are 2a and 2b in the X and Y directions, respectively. Receiver (x, y) can be put at any location inside the loop. The coordinate (x′, y′) is the position of the dipole, and the four boundaries of the loop are denoted by letters A, B, C and D, respectively. Theoretically, the total field contribution is the algebraic summation over all four boundaries. The field of rectangular loop can be expressed as an integral expression:

$$E_x = A + C \tag{8}$$

$$A = -\int_{-a}^{a}\frac{z\hat{}_0 I}{4\pi}\int_0^\infty \frac{2\lambda}{\lambda+u_1}J_0(\lambda r)d\lambda dx'$$

where, $r = \sqrt{(x-x')^2+(y-b)^2}$

$$C = -\int_{a}^{-a}\frac{z\hat{}_0 I}{4\pi}\int_0^\infty \frac{2\lambda}{\lambda+u_1}J_0(\lambda r)d\lambda dx'$$

where, $r = \sqrt{(x-x')^2+(y+b)^2}$.

The X-component of electric field is only excited by A and C; similarly, the Y-component of electric field is only excited by B and D

$$H_y = A + C \tag{9}$$

$$A = -\int_{-a}^{a}\frac{I}{4\pi}\int_0^\infty \frac{2\lambda u_1}{\lambda+u_1}J_0(\lambda r)d\lambda dx'$$

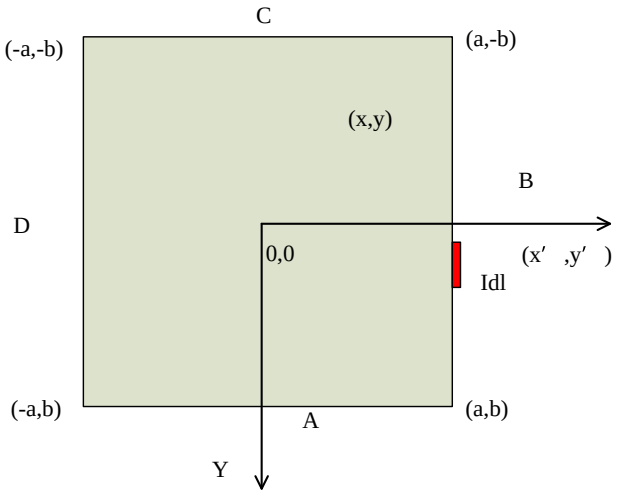

Fig. 2. Sketch map of rectangular loop.

where, $r = \sqrt{(x-x')^2 + (y-b)^2}$

$$C = -\int_{a}^{-a} \frac{I}{4\pi} \int_{0}^{\infty} \frac{2\lambda u_1}{\lambda + u_1} J_0(\lambda r) d\lambda dx'$$

where, $r = \sqrt{(x-x')^2 + (y+b)^2}$.

The Y-component of magnetic field is only excited by B and D. Similarly, the X-component of electric field is excited by A and C

$$Hz = A + B + C + D. \quad (10)$$

$$A = \int_{-a}^{a} \frac{Idl}{4\pi} \frac{|y-y'|}{r} \int_{0}^{\infty} (1 + r_{TE}) \frac{\lambda^2}{u_0} J_1(\lambda r) d\lambda dx'$$

where, $r = \sqrt{(x-x')^2 + (y-b)^2}$

$$B = \int_{-b}^{b} \frac{Idl}{4\pi} \frac{|x-x'|}{r} \int_{0}^{\infty} (1 + r_{TE}) \frac{\lambda^2}{u_0} J_1(\lambda r) d\lambda dy'$$

where, $r = \sqrt{(x-a)^2 + (y-y')^2}$

$$C = \int_{-a}^{a} \frac{Idl}{4\pi} \frac{|y-y'|}{r} \int_{0}^{\infty} (1 + r_{TE}) \frac{\lambda^2}{u_0} J_1(\lambda r) d\lambda dx'$$

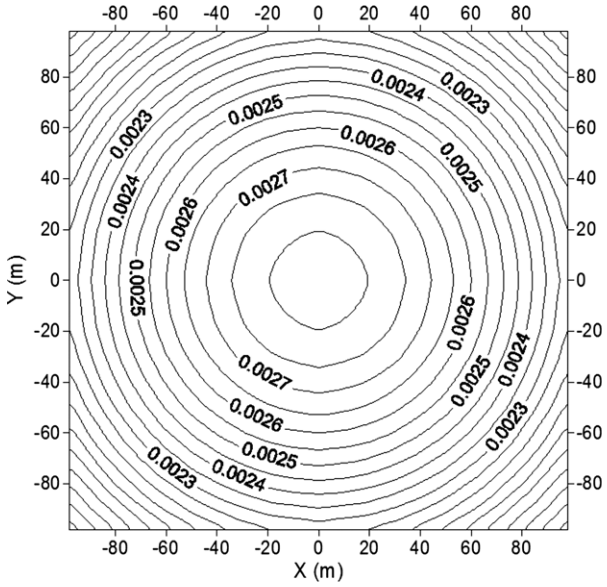

3-3 Hz

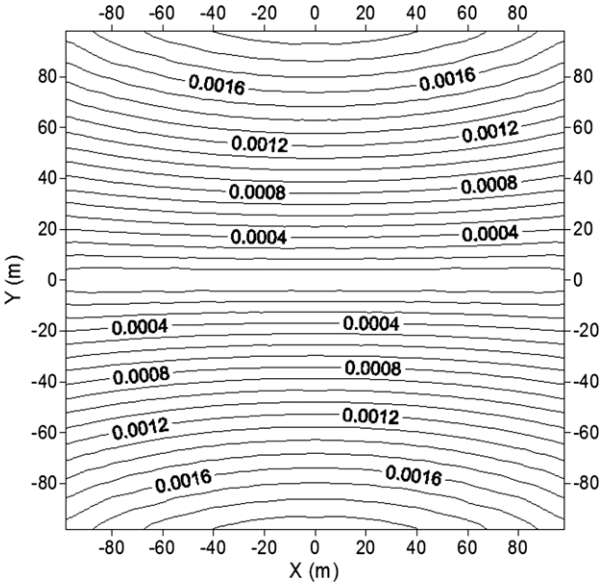

3-4 Ex

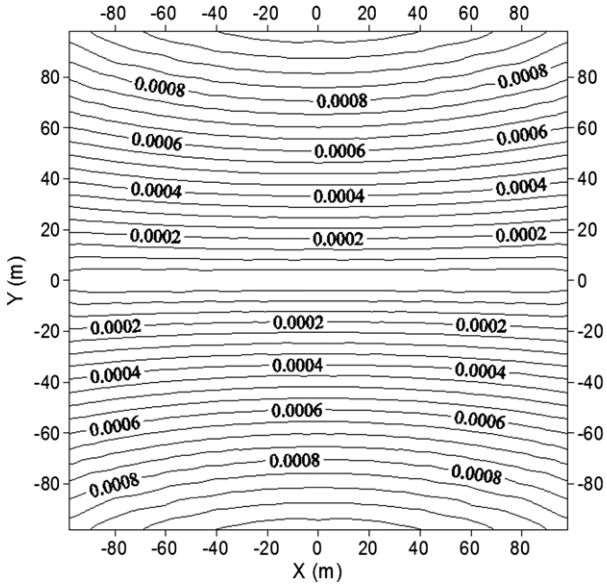

3-3 Hy

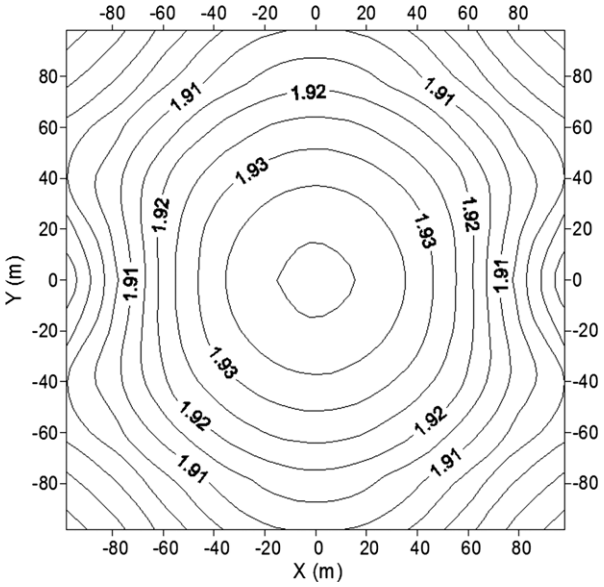

3-4 Ex/Hy

Fig. 3. Field distribution of Hz, Ex, Hy and Ex/Hy.

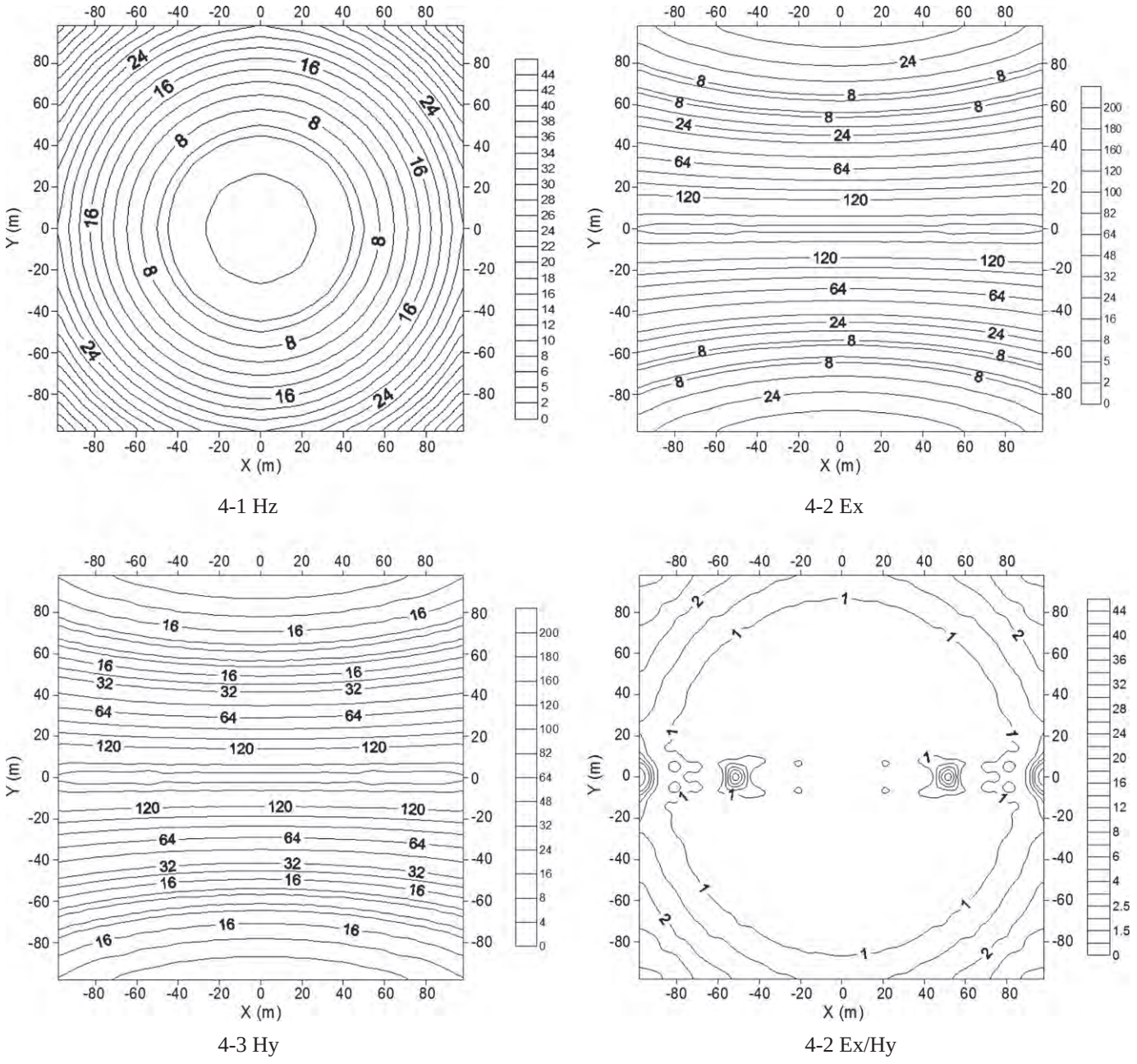

Fig. 4. Difference distribution of Hz, Ex, Hy and Ex/Hy.

Table 1
Ratio response of different resistivity at point (20, 60) for different times in square loop with side length 200.

Ratio response		t (s)				
		1.00E−05	1.00E−04	1.00E−03	1.00E−02	1.00E−01
σ (S/m)	1.00E−04	63.69	20.23	6.399	2.024	0.6399
	1.00E−03	19.34	6.369	2.023	0.6399	0.2024
	1.00E−02	4.676	1.934	0.6369	0.2023	0.06399
	1.00E−01	1.131	0.4676	0.1934	0.06369	0.02023
	1.00E+00	0.2735	0.1131	0.04676	0.01934	0.006369

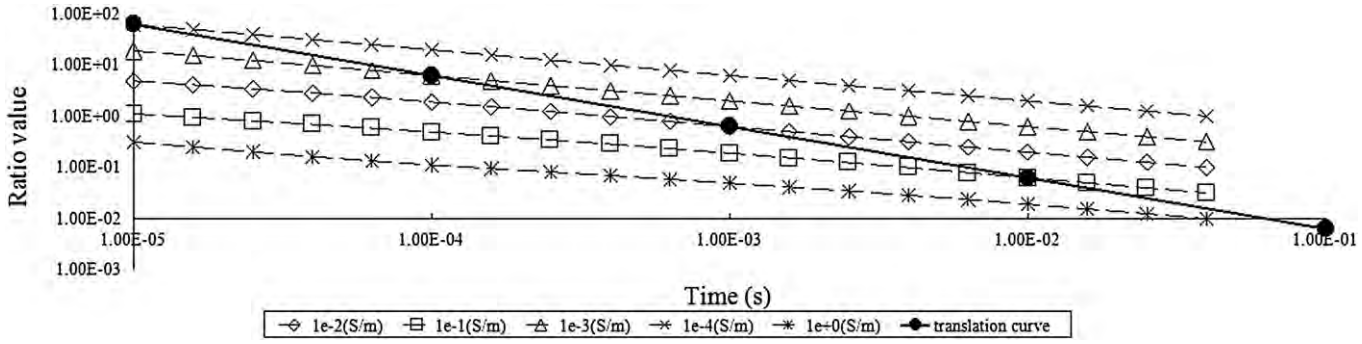

Fig. 5. Decay curves and translation line for different resistivity at point (20, 60).

where, $r = \sqrt{(x-x')^2 + (y+b)^2}$

$$D = \int_{-b}^{b} \frac{Idl}{4\pi} \frac{|x-x'|}{r} \int_0^{\infty} (1 + r_{TE}) \frac{\lambda^2}{u_0} J_1(\lambda r) d\lambda dy'$$

where, $r = \sqrt{(x+a)^2 + (y-y')^2}$.

During the calculation process, the Hankel and Cosine transform could be achieved by linear digital filtering (Anderson, 1979; Johansen and Sorensen, 1979).

3. Field distribution of rectangular loop

Loop size is set as 200 × 200 m carrying a current of 10 A. We calculate X-component of electric field, Y-component of magnetic field and vertical magnetic field using Eqs. (5)–(7), respectively. The distribution of the fields at 0.1 ms is shown in Fig. 3. Fig. 3-1 shows the distribution of vertical magnetic field, which is the central symmetric in loop. The response value decreases from center to side significantly, but the field is not evenly-distributed. Fig. 3-2and -3 displays the distribution of horizontal electric field and magnetic field, respectively. The response value increases by degrees and the interval between isolines is large. Initially, there is a sign change for X-component of electric field and Y-component of magnetic field with X-axis as divider line. For simplicity, only absolute values are shown here. From Fig. 3-2 and -3, we notice that the distribution of horizontal field is also not uniform. However, as shown in Fig. 3-4, the ratio response (Ex/Hy) distribution is both uniform and central symmetric. In addition, the isoline interval is very small.

In order to analyze the distribution uniformity of the field, we calculate the difference in loop. In particular, the loop center is used as the basic point to calculate the difference of vertical magnetic field; and we use a non-central point (20, 60) as the basic point to calculate the relative error of horizontal field and ratio response, due to the zero value of horizontal component at the central point. Similar to the field distribution, the difference distribution of vertical field is also central-symmetric. When the offset increases to be more than 40, the difference shows a significant increment of about 5%. This can be regarded as the upper limit of uniformity criterion. If the difference is larger than 5%, the field is not uniform. Thereby the uniform range of the vertical field is not larger than 16% of the loop area (shown in Fig. 4-1). Fig. 4-2 and -3 shows the difference distribution of horizontal electric and magnetic fields, and the error of horizontal field is far larger than that of vertical field. However, the uniform range where difference is less than 5% is much smaller. In contrast to the big difference of single component, the ratio field demonstrates difference that never exceeds 2%, and this meets the uniform condition.

Taking advantage of the uniformity of ratio field, any point in loop could be chosen as the basic point and this would lead to the definition of apparent resistivity, which can be used for any other point in loop.

Table 2
Intercepts for different resistivity at time of 1E−1 s.

σ (S/m)	p
1.00E−04	−0.69389
1.00E−03	−1.19379
1.00E−02	−1.69389
1.00E−01	−2.19389
1.00E+00	−2.69389

4. Translation definition of ratio apparent resistivity

Let $\sigma^* = K\sigma$, $t^* = Kt$.
If the response satisfies

$$\left(\frac{E_x}{H_y}\right)_{\sigma^*,t^*} = \frac{1}{K}\left(\frac{E_x}{H_y}\right)_{\sigma,t}, \tag{11}$$

the response has the property of translation and scaling (Wang, 2008).

Formula (11) shows that observation response for σ^* and t^* will be 1/K of that for σ and t. Take point (20, 60) as an example. We analyze the translation and scaling characteristic of ratio response and list them in Table 1.

As shown in Table 1, the calculated results verify the property of translation and scaling. In addition, we can plot double logarithmic figure using the half-space ratio response of different conductivities with the same device parameter. The decay curves of ratio response are shown in Fig. 5.

4.1. Translation algorithm definition of ratio apparent resistivity

The translation line of half-space ratio response is a straight line with the slope of 1:

$$\frac{\lg\left(\frac{E_x}{H_y}\right)_{\sigma^*,t^*} - \lg\left(\frac{E_x}{H_y}\right)_{\sigma,t}}{\lg t^* - \lg t} = -1.$$

Thus, the translation character can be represented by equation

$$\lg\left(\frac{E_x}{H_y}\right) = -\lg(t) + c \tag{12}$$

where, c is the intercept of the equation.

Table 3
Intercepts for different resistivity at time of 1E−5 s.

σ (S/m)	p
1.00E−03	−0.6314
1.00E−02	−1.2476
1.00E−01	−1.8640
1.00E+00	−2.4805

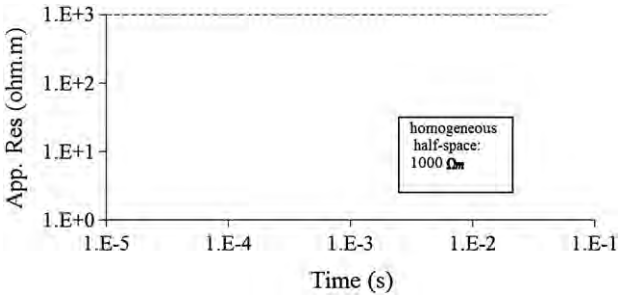

Fig. 6. Homogeneous half-space resistivity curve.

Likely, the ratio response for different resistivity should also satisfy the equation

$$\lg\left(\frac{E_x}{H_y}\right) = K \cdot \lg(t) + p \tag{13}$$

where, K is the slope; p denotes the intercept and is related to the resistivity of the earth.

In the upper right part of Table 1, the values of ratio response are geometric series. By taking the values at different times for $\sigma = 1e-4$S/m into the formula (13), the slope K can be obtained as $K = -1/2$. Then, for different resistivity at the time of 1E− 1 s, the intercepts are measured and shown in Table 2.

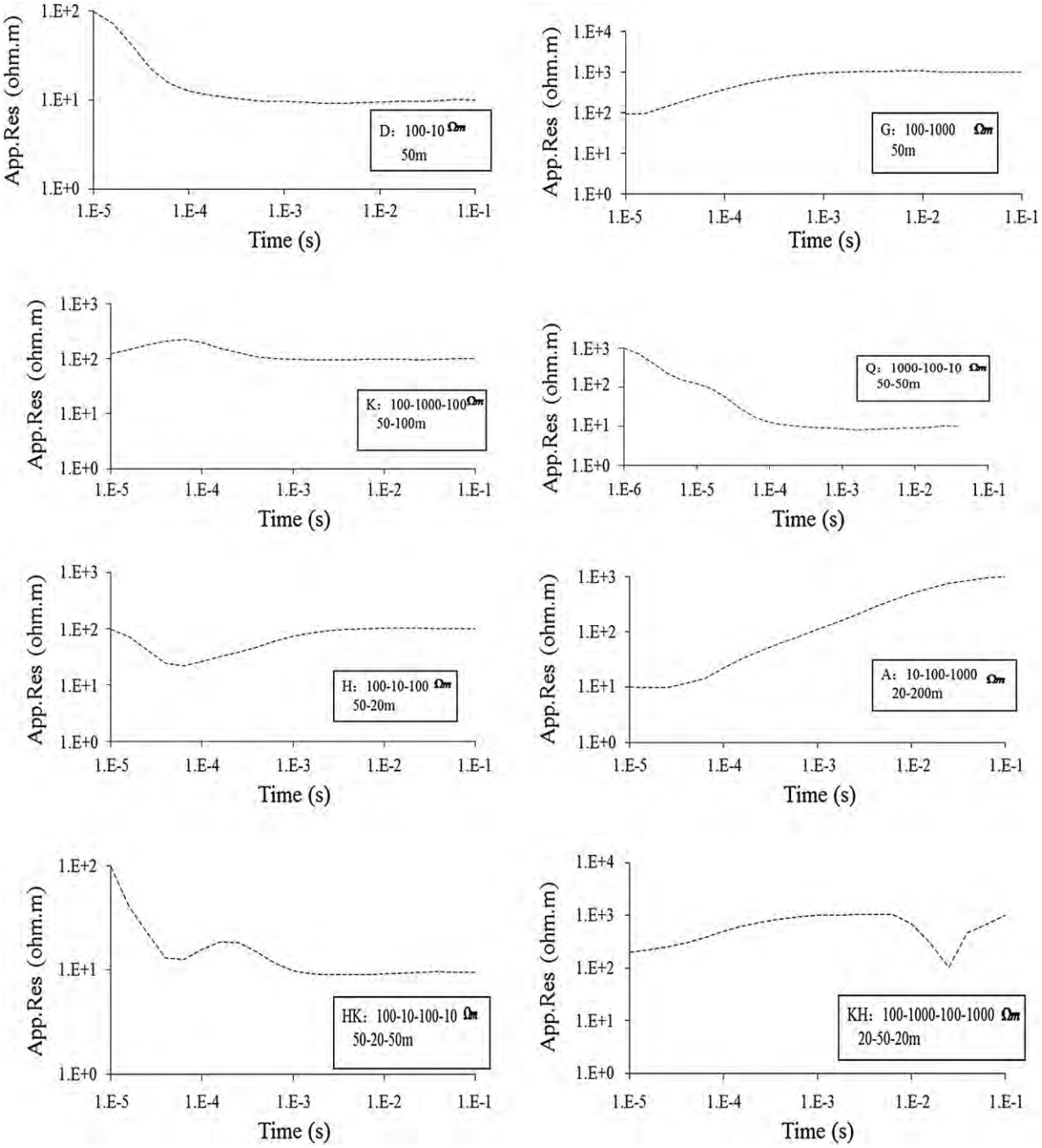

Fig. 7. Resistivity curves of layered models.

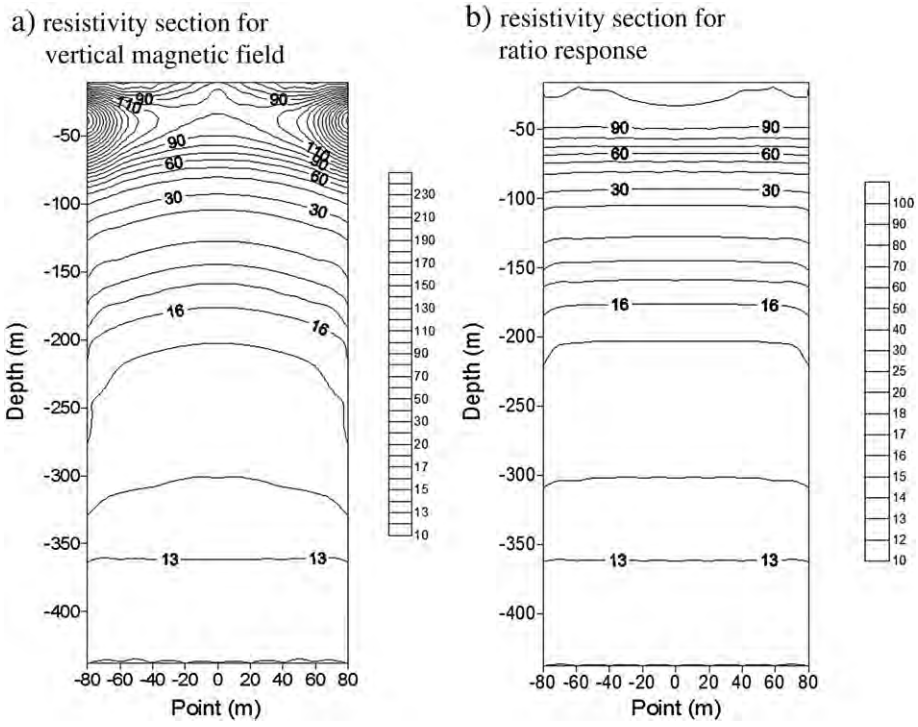

Fig. 8. Apparent resistivity sections for ratio response and vertical magnetic field.

Intercepts for different resistivity are arithmetic sequence:

$$p = -2.6938 - \frac{\lg(\sigma)}{2}. \tag{14}$$

So, for the upper right part, the resistivity can be obtained

$$\rho = 10^{5.3876}\left(\frac{E_x}{H_y}\right)^2 \cdot t. \tag{15}$$

Likely, in the lower left part of Table 1, take the values at different times for $\sigma = 1$S/m into the formula (13), the slope K can be obtained as $K = -0.3835$. Then, for different resistivity at the time of 1E− 5 s, the intercepts are computed and shown in Table 3.

Intercepts for different resistivity are arithmetic sequence:

$$p = -2.4805 - 0.6165\lg(\sigma). \tag{16}$$

Then, for the lower left part, the resistivity can be obtained

$$\rho = 10^{4.0236}\left(\frac{E_x}{H_y}\right)^{1.622} \cdot t^{0.622}. \tag{17}$$

For the observed or calculated response at given time t_0, let Eq. (15) equals (17), the inflection time t_1 will be obtained. If $t_0 = t_1$, both the two equations are right. If $t_0 < t_1$, Eq. (15) will be used. If $t_0 > t_1$, Eq. (17) will be used.

5. The theoretical model

In order to verify the value of formula (15) and (17) for all points in loop, we apply the formula to calculate the resistivity at point (60, 80) for different geo-electric models.

5.1. Homogeneous half-space model

The apparent resistivity curve (Fig. 6) fits well with the true resistivity, which shows the accuracy of ratio resistivity formula.

5.2. Layered model

For G and D model, apparent resistivity varies from the early time to the late time smoothly, either from high to low or from low to high. The apparent resistivity curve coincides with the real resistivity well. However, there are overestimates and underestimates at the interface between first layer and second layer, which always occur in the apparent resistivity calculation from induced voltage. Therefore, it implies that the false extreme values are caused by electric-field component.

For the three-layer models, the results of H and K show the true geo-electric model better than those of A and Q (Fig. 7). Specifically, apparent resistivity curve of H model can reach the real resistivity of inter-layer, while K model cannot. The explanation is that ratio apparent resistivity is more sensitive to low resistivity than high one, and this is also verified by the results of four-layer models. Therefore, the calculation of ratio resistivity is straightforward and does not need the time-

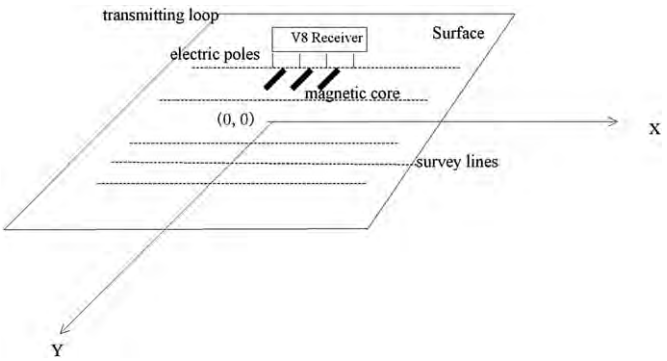

Fig. 9. TEM layout of survey lines and receiving system.

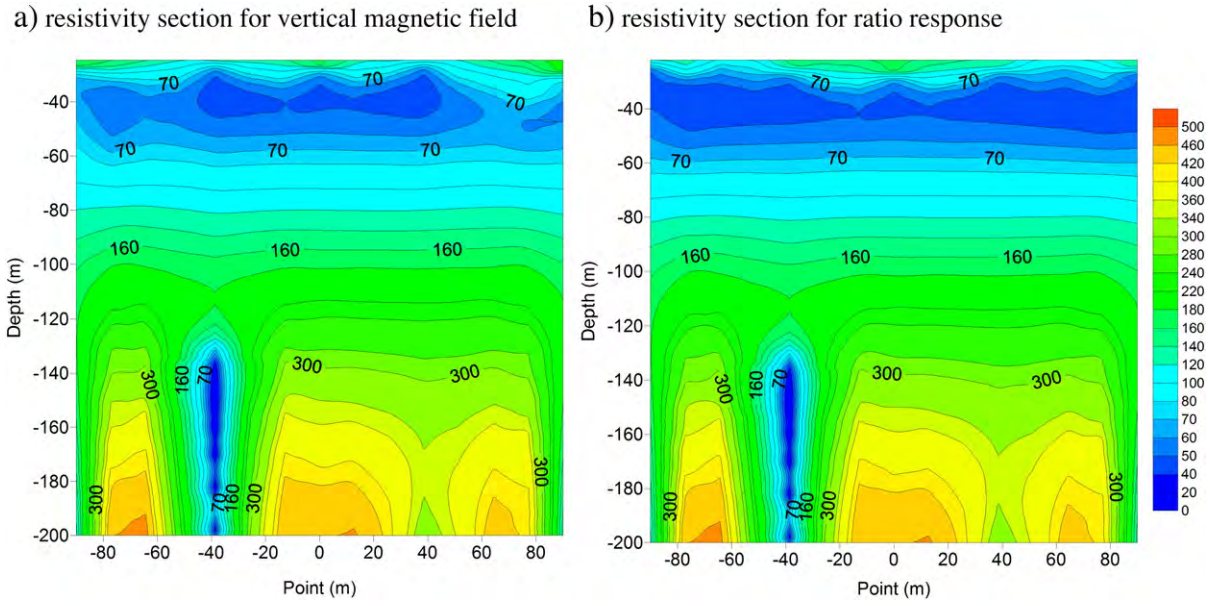

Fig. 10. Apparent resistivity sections for ratio response and vertical magnetic field.

consuming iteration. Meanwhile, the translation and scaling algorithm can be used for any point in loop because of the homogeneous property of ratio response.

5.3. Apparent resistivity section comparison

Formula (15) and (17) are used to calculate apparent resistivity for ratio response and compute the apparent resistivity for vertical magnetic field according to Christensen (1995). The geo-electric model parameters are:

$$\sigma_1 = 0.01\mathrm{S/m}, \sigma_2 = 0.1\mathrm{S/m}, \text{ and } h_1 = 100\mathrm{m}.$$

The converted depth can be calculated by the following equation (Spies and Eggers, 1986)

$$D(t) = \sqrt{\frac{t}{2\sigma\mu_0}}. \tag{18}$$

Fig. 8 shows the apparent resistivity sections for ratio response and vertical magnetic field. In Fig. 8a, apparent resistivity increases in the shallow layer and decreases with depth. However, there is an isoline trap in the shallow layer, which does not meet the real model. In contrast, in Fig. 8b, apparent resistivity decreases with depth, which satisfies the real model well.

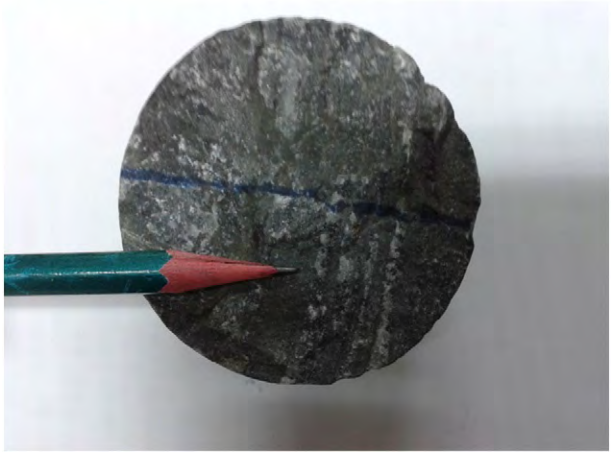

Fig. 11. Core from drill hole showing mineralization in the depth of −53 m at point −60 m.

6. Case study

We apply our method to one field example from Longhua iron ore in northern China. Longhua region is located in the north part of Hebei Province and North China craton, and Longhua iron ore deposit is the classical Precambrian banded iron ore (Zhang et al., 2004).

We choose the abnormal region of IP results as TEM survey area. The survey line length is 200 m. The Canadian-made V-8 electrical instrument was used. The transmitting loop 200 m by 200 m carrying 10 A current. The magnetic field receiving probe type is a SB-18K with the effective area 10000 m^2. The electric field is observed using electrodes. The magnetic probe is located in the middle of the electrode couple. The point space is 10 m and line space is 40 m. X-component of electric field, time-derivative of Y-component magnetic field and vertical magnetic field are observed. Unlike the CSAMT configuration, each Y-component of magnetic field is corresponding to one X-component of electric field (Fig. 9). In practice, the induced voltage was observed through magnetic probe, which is not the required magnetic field in Eqs. (15) and (17). Therefore, we need to transfer the induced voltage into magnetic field by Xu et al. (2008). The observed data of every time is an average of decay window. So, the magnetic field at time t_i can be obtained by integration of induced voltage from last time to the actual time t_i. In the integrating process, there will be a key parameter, i.e., integral constant, which is corresponding to the magnetic field at last time. For late-time data, the induced voltage and time satisfy the linear relation on double logarithmic coordinates and the slope is smaller than −1. So, the integral constant can be obtained using the linear regression based on the several late-time data. Then, substitute the integral constant into the integral expression and get the magnetic field.

Fig. 10 shows one typical apparent resistivity sections for ratio response and vertical magnetic field. Receivers are located at points of −75 m, −45 m, −15 m, 15 m, 45 m and 75 m. There is a low-resistivity anomaly from point −50 m to 40 m in the apparent resistivity section for vertical magnetic field (Fig. 10a), while the anomaly for ratio response exists through the total line (Fig. 10b), which is consistent with the real geo-electric information. Using the apparent resistivity for ratio response will provide more information about the shallow

area compared to the traditional definition of apparent resistivity of vertical magnetic field.

Some boreholes are drilled in the anomaly area with low resistivity. Fig. 11 shows one drilling core in the depth of −53 m at point −60 m. The borehole survey shows that the iron ore mineralization is obvious. So, the apparent resistivity near the depth of −53 m should be very low-resistivity, which is more consistent with the resistivity section for ratio response.

7. Conclusions

This paper first analyzes the response of electric dipole, which can be divided into current part and grounded part. Then the integral expression is simplified to calculate the three-component field of any point in loop. The ratio response in loop is stronger than that of single component. According to the translation and scaling properties of decay curve for different resistivity, an explicit expression of apparent resistivity is presented, which can be used for any point in loop (except axis). The translation algorithm avoids the time-consuming iteration and achieves the computation by solving a non-linear equation that is both computational efficient and accurate.

Acknowledgments

This work is supported by Chinese National Programs for Fundamental Research and Development (No. 2012CB416605), the National Natural Science Foundation of China (No. 41174090), and R&D of Key Instruments and Technologies for Deep Resources Prospecting (the National R&D Projects for Key Scientific Instruments), Grant No. ZDYZ2012-1-05. Finally, the authors would like to thank two reviewers, Prof. Farquharson and one anonymous reviewer, the editor for many helpful comments and suggestion, and Dr. Di H. B. for grammar and English expression.

References

Anderson, 1979. Numerical integral of related Hankel transforms of order 0 and 1 adaptive digital filtering. Geophysics 44, 1287–1305.
Christensen, N.B., 1995. 1D imaging of central loop transient electromagnetic soundings. J. Environ. Eng. Geophys. 2 (1), 53–60.
Johansen, H.K., Sorensen, K., 1979. Fast Hankel transforms. Geophys. Prospect. 27, 876–901.
Kauahikaua, J., 1978. Electromagnetic fields about a horizontal electric wire source of arbitrary length. Geophysics 43 (5), 1019–1022.
Lee, T., Lewis, R., 1974. Transient response of a large loop on a layered ground. Geophys. Prospect. 22, 430–444.
Li, J.P., Li, T.L., Zhao, X.F., et al., 2007. Study on the TEM all-time apparent resistivity of arbitrary shape loop source over the layered medium. Prog. Geophys. 22 (6), 1777–1780 (in Chinese).
Qi, Z.P., Li, X., Guo, W.B., et al., 2011. Definition of apparent resistivity for horizontal-component of transient electromagnetic method. J. China Coal Soc. 36, 88–93 (Sup).
Raiche, A.P., Spies, B.R., 1981. Coincident-loop transient electromagnetic master curves for interpretation of two-layer earths. Geophysics 46, 53–64.
Shi, X.X., Yan, S., Fu, J.M., et al., 2009. Improvement for interpretation of central loop transient electromagnetic method. Chin. J. Geophys. 52 (7), 1931–1936 (in Chinese).
Spies, B., Eggers, D., 1986. The use and misuse of apparent resistivity in electromagnetic methods. Geophysics 51 (7), 1462–1471.
Spies, B.R., Raiche, A.P., 1980. Calculation of apparent conductivity for the transient electromagnetic (coincident loop) method using Hp-67 calculator. Geophysics 45 (7), 1197–1204.
Wang, H.J., 2008. Time domain transient electromagnetic all time apparent resistivity translation algorithm. Chin. J. Geophys. 51 (6), 1936–1942.
Ward, S.H., Hohmann, G.W., 1991. Electromagnetic theory for geophysical exploration. In: Nabighian, N. (Ed.), Electromagnetic Methods in Applied Geophysics. Society of Exploration Geophysics, Tusla, Oklahama, pp. 121–223.
Xu, J.R., Li, A.Y., Yang, S., 2008. Calculation of transient magnetic field and all time apparent resistivity based on central loop TEM. Geol. Prospect. 44 (6), 62–68.
Xue, G.Q., Bai, C.Y., Yan, Y., 2012. Deep sounding TEM investigation method based on a modified fixed central-loop system. J. Appl. Geophys. 76, 23–32.
Zhang, S., Zhao, Y., Song, B., et al., 2004. The late Paleozoic gneissic granodiorite pluton in early Precambrian high-grade metamorphic terrains near Longhua County in northern Hebei Province, North China: result from zircon SHRIMP U-Pb dating and its tectonic implications. Acta Petrol. Sin. 20, 621–626 (in Chinese with English abstract).
Zhou, N.N., Xue, G.Q., Li, M.F., et al., 2011. Response of large-loop TEM based on approximation of electric dipole. Coal Geol. Explor. 4 (39), 49–54.